

A Comprehensive Study of PAPR Reduction Techniques for Deep Joint Source Channel Coding in OFDM Systems

Maolin Liu^{1,2}, Wei Chen^{1,2,3}, Jialong Xu^{1,2}, Bo Ai^{1,2,4}

¹State Key Laboratory of Advanced Rail Autonomous Operation, Beijing Jiaotong University, China

²School of Electronic and Information Engineering, Beijing Jiaotong University, Beijing, China

³Key Laboratory of Railway Industry of Broadband Mobile Information Communications

⁴Beijing Engineering Research Center of High-speed Railway Broadband Mobile Communications

Corresponding author: *Wei Chen*

Abstract—Recently, deep joint source channel coding (DJSCC) techniques have been extensively studied and have shown significant performance with limited bandwidth and low signal to noise ratio. Most DJSCC work considers discrete-time analog transmission, while combining it with orthogonal frequency division multiplexing (OFDM) creates serious high peak-to-average power ratio (PAPR) problem. This paper conducts a comprehensive analysis on the use of various OFDM PAPR reduction techniques in the DJSCC system, including both conventional techniques such as clipping, companding, SLM and PTS, and deep learning-based PAPR reduction techniques such as PAPR loss and clipping with retraining. Our investigation shows that although conventional PAPR reduction techniques can be applied to DJSCC, their performance in DJSCC is different from the conventional split source channel coding. Moreover, we observe that for signal distortion PAPR reduction techniques, clipping with retraining achieves the best performance in terms of both PAPR reduction and recovery accuracy. It is also noticed that signal non-distortion PAPR reduction techniques can successfully reduce the PAPR in DJSCC without compromise to signal reconstruction.

Index Terms—Joint source channel coding, OFDM, PAPR

I. INTRODUCTION

Deep learning (DL) is considered as a promising technique in solving wireless communication problems in recent years [1]–[4]. In particular, the deep joint source channel coding (DJSCC) approach [3], [4] has been demonstrated to be more effective than the traditional split source channel coding (SSCC) technique, with lower distortion, simpler design and computation, and the elimination of the “cliff effect”. However, due to the randomness of the generated symbols, DJSCC poses a serious high peak-to-average power ratio (PAPR) problem when combined with orthogonal frequency division multiplexing (OFDM). High PAPR results in in-band distortion and out-of-band radiation, which are caused by the nonlinearity of the radio transmitter’s high-power amplifier (HPA). Moreover, the detection efficiency of OFDM receivers is particularly sensitive to nonlinear devices such as digital-to-analog converters (DACs) and HPA.

Various PAPR reduction techniques have been proposed and successfully used in engineering practice. PAPR reduction techniques can be classified into signal distortion and non-

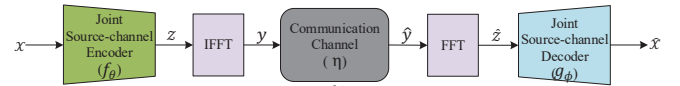


Fig. 1: The OFDM-based DJSCC system.

distortion classes depending on whether they introduce distortion to the original signal or not. The signal distortion PAPR reduction techniques mainly include clipping [7], clipping filtering [8], peak-adding windowing [9], peak-canceling [10] and companding [11]. Signal non-distortion PAPR reduction techniques include precoding [12], selective mapping (SLM) [13], partial transmit sequence (PTS) [13], interleaving [14], tone reservation [15], tone injection [15], active constellation expansion [16], and constellation reshaping [17]. In addition to conventional schemes, some DL-based PAPR reduction techniques have recently been proposed [18], whose main idea is to model and train the OFDM system end-to-end using a neural network model, leading to low PAPR output.

Few investigations have been conducted into the problem of high PAPR in OFDM-based DJSCC systems. These works only consider signal distortion PAPR reduction methods, and there is no investigation on the effectiveness of signal non-distortion methods for DJSCC as far as we know. Furthermore, even for signal distortion methods, existing work focuses mainly on the clipping technique [5], [6]. In view of the fact that there exist many PAPR reduction methods, no work has comprehensively studied and compared different methods for DJSCC. To this end, in this paper, we evaluate the performance of various PAPR reduction techniques for OFDM in DJSCC systems. The coverage of the PAPR reduction techniques investigated in this paper and the related literature [5], [6] are summarized in Table I.

II. SYSTEM MODEL

A. Deep joint source-channel coding

Considering a point-to-point DJSCC based OFDM system for signal transmission as shown in Fig. 1, the encoder maps

TABLE I: Comparison of the PAPR reduction techniques for DJSCC studied in literature and our paper.

Category	PAPA reduction technique	[5]	[6]	Ours
Conventional signal distortion technique	Clipping	✓	✓	✓
	Companding			✓
DL-based signal distortion technique	PAPR Loss		✓	✓
	Clipping with retrain	✓	✓	✓
Signal non-distortion technique	SLM			✓
	PTS			✓

the n -dimensional input $\mathbf{x} \in \mathbb{R}^n$ to a k -dimensional complex-valued feature $\mathbf{z} \in \mathbb{C}^k$, and \mathbf{z} satisfies the average power constraint $\frac{1}{k} \mathbb{E}(\mathbf{z}\mathbf{z}^*) \leq 1$, where \mathbf{z}^* represents the complex conjugate of \mathbf{z} . The bandwidth to signal ratio is defined as $R = \frac{k}{n}$. The encoding function $f_\theta: \mathbb{R}^n \rightarrow \mathbb{C}^k$ is a neural network with a set of parameters θ , and the encoding process can be represented as $\mathbf{z} = f_\theta(\mathbf{x})$. The encoded symbol sequence \mathbf{z} is transformed by inverse fast Fourier transform (IFFT) into a time domain channel input \mathbf{y} and sent through an additive Gaussian white noise channel (AWGN). The channel output $\hat{\mathbf{y}} \in \mathbb{C}^k$ can be expressed as $\hat{\mathbf{y}} = \mathbf{y} + \mathbf{n}$, where $\mathbf{n} \in \mathbb{C}^k$ is an independent identically distributed Gaussian noise vector with mean 0 and variance σ^2 .

The received signal is transformed by fast Fourier transform (FFT) to generate the frequency domain signal $\hat{\mathbf{z}}$, which is used as the input of the decoder. The decoder maps $\hat{\mathbf{z}}$ to $\hat{\mathbf{x}} \in \mathbb{R}^n$ that is the estimation of the original vector $\mathbf{x} \in \mathbb{R}^n$. Similarly to the encoder, the decoder function $g_\phi: \mathbb{C}^k \rightarrow \mathbb{R}^n$ exploits a neural network with a set of parameters ϕ . The decoding process can be expressed as:

$$\hat{\mathbf{x}} = g_\phi(\hat{\mathbf{z}}) = g_\phi(\text{FFT}(f_\theta(\text{IFFT}(\mathbf{x}))) + \mathbf{n}). \quad (1)$$

The distortion between the original signal \mathbf{x} and the reconstructed signal $\hat{\mathbf{x}}$ can be expressed as $d(\mathbf{x}, \hat{\mathbf{x}}) = \frac{1}{n} \sum_{i=1}^n (x_i - \hat{x}_i)^2$, where x_i and \hat{x}_i represent the i th elements of \mathbf{x} and $\hat{\mathbf{x}}$, respectively. With a fixed bandwidth to signal ratio R , the DJSCC design aims to find the encoder and decoder parameters θ^* and ϕ^* that minimize the end-to-end distortion as follows:

$$(\theta^*, \phi^*) = \arg \min_{\theta, \phi} \mathbb{E}_{p(\mathbf{x}, \hat{\mathbf{x}})} [d(\mathbf{x}, \hat{\mathbf{x}})], \quad (2)$$

where $p(\mathbf{x}, \hat{\mathbf{x}})$ is the joint probability distribution of the original and reconstructed signal. We model the encoder and decoder using the neural network structure in [3] for image transmission.

B. Peak-to-average power ratio in OFDM

The PAPR in OFDM is defined as the ratio of the peak power to the average power of the signal, and the PAPR of a discrete OFDM signal can be expressed as follows:

$$\text{PAPR}(\text{dB}) = 10 \log_{10} \frac{\max_k y_k^2}{E[\|\mathbf{y}\|_2^2]} \quad (3)$$

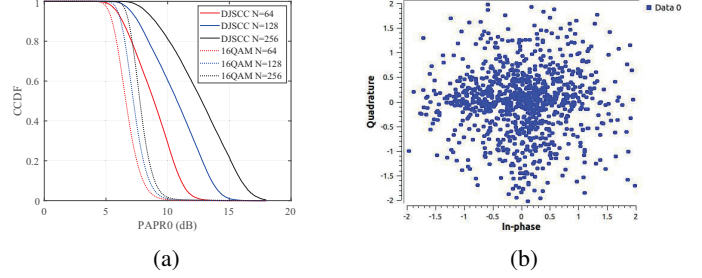


Fig. 2: (a) PAPR performance comparison between DJSCC and 16QAM. (b) DJSCC constellation diagram.

where the denominator $E[\cdot]$ denotes the expectation, y_k denotes the k -th sample of the time-domain OFDM symbol, $k \in \{0, 1, 2, \dots, N-1\}$. The superposition of multiple carrier signals leads to large peaks in the OFDM signal, and this phenomenon is more severe as the number of subcarriers increases. The performance of PAPR is usually evaluated using the complementary cumulative distribution function (CCDF) of PAPR, i.e., $CCDF(\text{PAPR0}) = P\{\text{PAPR} > \text{PAPR0}\}$.

We evaluate the PAPR performance of DJSCC and 16QAM in the OFDM system with different numbers of subcarriers, and the result is shown in Fig. 2a. It can be seen that the PAPR values gradually increase as the number of carriers increases, but DJSCC has a larger PAPR, and the increase in the number of carriers intensifies this phenomenon. This can be explained by the fact that the DJSCC discrete-time analog transmission generates scattered and random modulation constellation points as shown in Fig. 2b, which are more likely to generate large peak power symbols, and the superposition of multiple carriers further exacerbates this phenomenon, thus producing a higher PAPR.

III. PAPR REDUCTION TECHNIQUES

In this section, conventional PAPR reduction techniques and deep learning-based PAPR reduction techniques are introduced.

A. Conventional signal distortion techniques

1) Clipping

Clipping simply crops the signal according to a set threshold, reducing the signal peak while retaining most of the low

amplitude signal samples, the clipped signal can be expressed as:

$$y_{clip}(n) = \begin{cases} y[n]e^{j\phi[n]}, & y[n] < \rho\sqrt{P} \\ \rho\sqrt{P}e^{j\phi[n]}, & y[n] \geq \rho\sqrt{P} \end{cases} \quad (4)$$

where $y[n]$ represents the OFDM time-domain symbolic sample sequence with phase $\phi[n]$, and the phase of the signal does not change before and after limiting. ρ represents the clipping rate (CR), defined as the ratio of the limiting threshold amplitude to the root-mean-square of the original signal symbols.

2) μ -law Companding

The companding method uses a companding function to compress the large-amplitude signal of the OFDM time domain signal and expand the small-amplitude signal, thus reducing the PAPR of the signal. Unlike the clipping method, the companding method is able to recover the signal to some extent by an inverse companding function, and the recovery effect is related to the choice of the companding function.

The μ -law companding function is expressed as:

$$z_{n,k} = \frac{V y_{n,k}}{\ln(1 + \mu)|y_{n,k}|} \ln\left(1 + \frac{\mu}{V}|y_{n,k}|\right) \quad (5)$$

where $y_{n,k}$ represents the k -th sample of the n -th OFDM symbol of the transmit signal. V denotes the magnitude mean of the time-domain OFDM symbols, and $|y_{n,k}|$ is the modulus of complex samples $y_{n,k}$. μ is a constant that controls the degree of compression.

The inverse companding function applied at the receiver is expressed as:

$$y_{n,k}' = \frac{V' z_{n,k}'}{\mu |z_{n,k}'|} e^{\left(\frac{|z_{n,k}'| \ln(1 + \mu)}{V'}\right) - 1} \quad (6)$$

where V' denotes the average amplitude of the received signal $z_{n,k}'$.

B. Conventional signal non-distortion techniques

1) SLM

The SLM system block diagram is shown in Fig. 3. The frequency-domain signal X is copied into V copies denoted as $\{X_1, X_2, X_3, \dots, X_{V-1}, X_V\}$, and each copy is multiplied by a sequence of phase factors $p_v, v \in 1, 2, \dots, V$, where a single phase factor $p_v^{(k)} = \exp(j\varphi), \varphi \in [0, 2\pi]$. Then we have the phase-transformed signal set X' and the time-domain OFDM signal set Y by the IFFT transform. The selector selects from the set of signals Y to obtain the smallest PAPR for transmission. The group sequence of the selected signal is transmitted to the receiver as additional information together with the signal, and the receiver can recover the original signal by finding the corresponding phase factor sequence according to the sequence number. In this process, SLM does not bring additional distortion to the original signal.

2) PTS

PTS is very similar to SLM and its structure is illustrated in Fig. 4. A modulated symbol sequence $X = [X_1, X_2, X_3, \dots, X_{N-1}, X_N]$, where N denotes the number of subcarriers, is partitioned into V parts. The number of valid

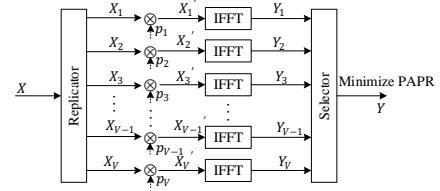


Fig. 3: SLM system framework.

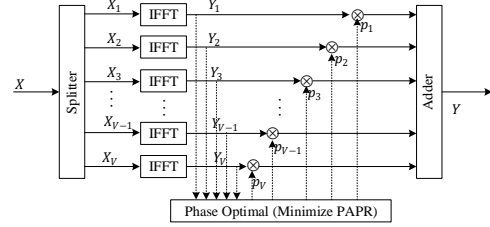


Fig. 4: PTS system framework.

data in each part is N/V , and the rest of the positions are filled with zeros to form a data block of length N , and then N -point IFFT transform is applied to the data block to generate the time domain signal. A random sequence of V phase factors of length N is generated $p_v, v \in 1, 2, \dots, V$, where a single phase factor $p_v^{(k)} = \exp(j\varphi), \varphi \in [0, 2\pi], k \in 1, 2, \dots, N$, usually chosen among $[\pm 1, \pm 1j]$. The phase factor sequence and the corresponding signal of each branch are weighted and summed, and the PAPR is calculated. After M times of the same operation, the phase factor sequence with the smallest PAPR is selected as the final phase factor sequence to generate the time-domain emission signal, which would lead to the reduction of PAPR.

C. Deep learning-based techniques

1) PAPR Loss

According to [18], adding PAPR to the loss function of a neural network can learn a network model with low PAPR output. To reduce the distortion between the output and input of the network, the loss function L_1 of the original DJSCC can be expressed as:

$$L_1 = \|\mathbf{x} - g(\text{FFT}(\text{IFFT}(f(\mathbf{x}, \theta)) + \mathbf{n}), \phi)\|_2 \quad (7)$$

To reduce the PAPR, the loss function L_2 can be expressed as:

$$L_2 = \mathbb{E}[PAPR\{\text{IFFT}(f(\mathbf{x}, \theta))\}] \quad (8)$$

where \mathbb{E} denotes the mean value.

In order to minimize both distortion and PAPR, the new DJSCC loss function is constructed by combining the loss functions L_1 and L_2 denoted as:

$$L = L_1 + \lambda L_2 \quad (9)$$

where λ denotes the weight to trade-off the two penalties. A larger λ means that the learning is more biased towards reducing the PAPR and vice versa for reducing the distortion between the reconstructed signal and the original signal.

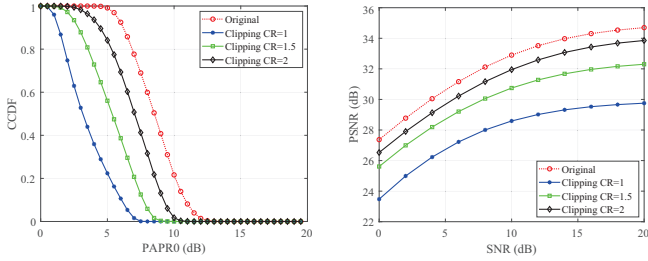


Fig. 5: Performance of PAPR (left) and PSNR (right) of clipping in DJSCC.

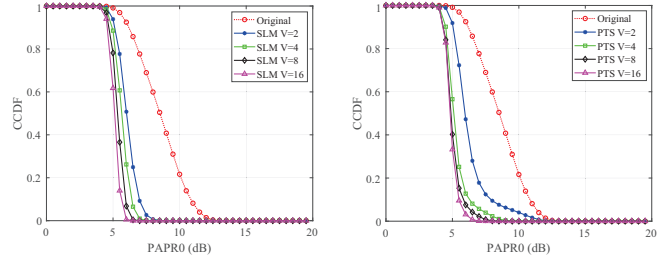


Fig. 7: Performance of PAPR of SLM (left) and PTS (right) in DJSCC.

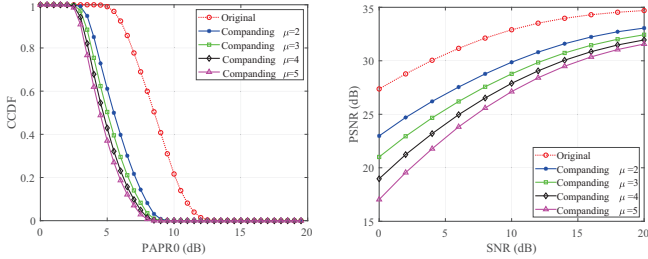


Fig. 6: Performance of PAPR (left) and PSNR (right) of companding in DJSCC.

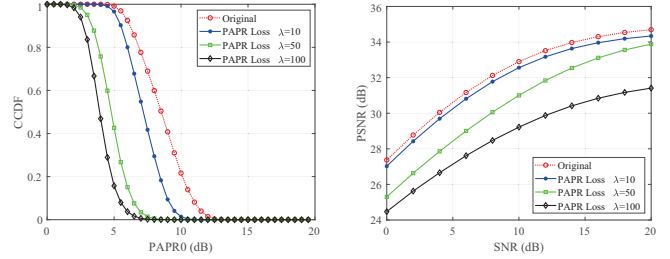


Fig. 8: Performance of PAPR (left) and PSNR (right) of ‘‘PAPR Loss’’ in DJSCC.

2) Clipping with retraining

Deep learning can learn the output of a network with certain features through a nonlinear function in the network. Therefore, clipping can be added as a nonlinear function to the network in the training process to further improve the performance. The clipping function can be expressed as follows:

$$y_{clip}[n] = y[n] \left(1 - \frac{ReLU(|y[n]| - \rho \bar{y}[n])}{|y[n]| + \gamma} \right) \quad (10)$$

where $y[n]$ represents the IFFT transformed signal of the joint encoder output, ρ represents the clipping ratio, $|y[n]|$ represents the mode of the complex symbol, $\bar{y}[n]$ represents the average amplitude of the signal, and γ represents a constant much smaller than 0 to avoid the denominator being 0.

IV. EXPERIMENTAL RESULTS

We used tensorflow and its high-level API Keras to learn the encoder and decoder of DJSCC, and an Adam optimizer with a learning rate of 10^{-4} and a batch size of 128 was considered in the training. ImageNet [19] was used as the training dataset, which contains more than 14 million images with more than 21,000 categories. We train the model with the SNR drawn from a uniform distribution in the range of $[0, 20]$ dB. For simplicity, the neural network is trained under the AWGN channel, and extension to the fading channel is trivial. The Kodak dataset was used to evaluate DJSCC performance, which contains 24 images of size 768×512 . Each image in the Kodak dataset is transmitted 10 times with different noise instances. In all experiments, the number of OFDM subcarriers is 64, and the DJSCC bandwidth to signal ratio is set to 1/6.

Fig. 5 shows the PAPR and image peak signal to noise ratio (PSNR) performance of DJSCC after conventional clipping. It can be seen that the PAPR performance of DJSCC has improved significantly after clipping, and the improvement increases as the CR decreases. However, the signal distortion generated by clipping also leads to the degradation of PSNR performance, and the magnitude of the degradation increases with the decrease in CR. The performance of DJSCC using the companding method is shown in Fig. 6. It can be seen that the PAPR performance of DJSCC after companding has improved significantly, but the PSNR performance has decreased. Furthermore, the improvement in PAPR increases with increasing μ , while the quality of image reconstruction decreases with increasing μ . We assume that the phase factor sequences of SLM and PTS are transmitted without errors, then they do not cause distortion to the signal, so we only observe the PAPR reduction performance of both as shown in Fig. 7. It can be seen that both methods can inhibit PAPR in DJSCC, and the suppression level increases with the increase of V .

Fig. 8 shows the performance of DJSCC after adding PAPR to the loss function. It can be seen that this method can suppress the PAPR of DJSCC, but it also reduces PSNR performance. Moreover, both the PAPR of DJSCC and the reconstruction quality of the images decrease with increasing penalty factor λ . Fig. 9 demonstrates the PAPR and PSNR performance by adding the clipping process to the DJSCC training. It can be seen that this method reduces the PAPR of DJSCC while degrading the PSNR performance. The decrease in PSNR is smaller compared to the conventional clipping method with the same CR, especially when the CR is larger.

We evaluate the PAPR and PSNR performance of all the

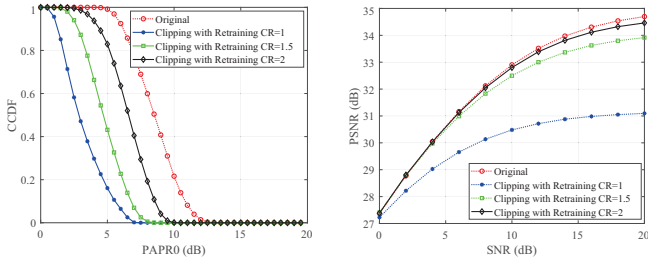


Fig. 9: Performance of PAPR (left) and PSNR (right) of “Clipping with Retraining” in DJSCC.

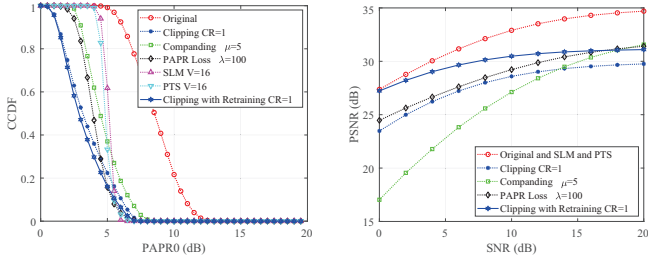


Fig. 10: Performance comparison of all PAPR reduction techniques in DJSCC.

methods mentioned in the previous section, shown in Fig. 10. Among signal distortion PAPR reduction techniques, the clipping with retraining achieves the best PSNR performance, especially at low SNRs. However, in conventional SSCC with digital modulation, the performance of the companding method is superior to that of the clipping method, especially at higher order modulations [20]. In addition, clipping with retraining does not require any modification of the network model and does not add excessive computational complexity. Furthermore, we also find that signal non-distortion PAPR reduction techniques, i.e., SLM and PTS, can successfully reduce the PAPR in DJSCC without compromise to signal reconstruction.

V. CONCLUSION

In this paper, we investigate PAPR reduction techniques for DJSCC-based OFDM system, including conventional PAPR reduction techniques and DL-based PAPR reduction techniques. Simulation results show that although the conventional PAPR reduction techniques can be applied to DJSCC, the performance in DJSCC is different to that of conventional SSCC, e.g., the performance of clipping is better/worse than companding in DJSCC/SSCC. Moreover, for signal distortion PAPR reduction techniques, clipping with retraining achieves the best performance in terms of both PAPR reduction and recovery accuracy. Furthermore, signal non-distortion PAPR reduction techniques, i.e., SLM and PTS can successfully reduce the PAPR in DJSCC without compromise to signal reconstruction.

REFERENCES

- [1] Y. Bai, W. Chen, F. Sun, B. Ai, and P. Popovski, “Data-driven compressed sensing for massive wireless access,” *IEEE Communications Magazine*, vol. 60, no. 11, pp. 28–34, 2022.
- [2] Y. Bai, W. Chen, B. Ai, Z. Zhong, and I. J. Wassell, “Prior information aided deep learning method for grant-free noma in mmTc,” *IEEE Journal on Selected Areas in Communications*, vol. 40, no. 1, pp. 112–126, 2022.
- [3] E. Boursoulatzé, D. B. Kurka, and D. Gündüz, “Deep joint source-channel coding for wireless image transmission,” *IEEE Transactions on Cognitive Communications and Networking*, vol. 5, no. 3, pp. 567–579, 2019.
- [4] J. Xu, B. Ai, W. Chen, A. Yang, P. Sun, and M. Rodrigues, “Wireless image transmission using deep source channel coding with attention modules,” *IEEE Transactions on Circuits and Systems for Video Technology*, vol. 32, no. 4, pp. 2315–2328, 2021.
- [5] M. Yang, C. Bian, and H.-S. Kim, “Deep joint source channel coding for wireless image transmission with ofdm,” in *ICC 2021-IEEE International Conference on Communications*, pp. 1–6, IEEE, 2021.
- [6] Y. Shao and D. Gunduz, “Semantic communications with discrete-time analog transmission: A papr perspective,” *IEEE Wireless Communications Letters*, vol. 12, no. 3, pp. 510–514, 2022.
- [7] R. O’Neill and L. B. Lopes, “Envelope variations and spectral splatter in clipped multicarrier signals,” in *Proceedings of 6th International Symposium on Personal, Indoor and Mobile Radio Communications*, vol. 1, pp. 71–75, IEEE, 1995.
- [8] X. Li and L. J. Cimini, “Effects of clipping and filtering on the performance of ofdm,” in *1997 IEEE 47th Vehicular Technology Conference. Technology in Motion*, vol. 3, pp. 1634–1638, IEEE, 1997.
- [9] M. Pauli and P. Kuchenbecker, “On the reduction of the out-of-band radiation of ofdm-signals,” in *ICC’98. 1998 IEEE International Conference on Communications. Conference Record. Affiliated with SUPERCOMM’98 (Cat. No. 98CH36220)*, vol. 3, pp. 1304–1308, IEEE, 1998.
- [10] L. Wang, K. Cho, D. Yoon, and S. K. Park, “A recoverable peak cancellation technique for papr reduction of ofdm signals,” in *2006 International Conference on Communications, Circuits and Systems*, vol. 2, pp. 1124–1127, IEEE, 2006.
- [11] X. Wang, T. T. Tjhung, and C. S. Ng, “Reduction of peak-to-average power ratio of ofdm system using a companding technique,” *IEEE transactions on broadcasting*, vol. 45, no. 3, pp. 303–307, 1999.
- [12] P. Fan and X.-G. Xia, “Block coded modulation for the reduction of the peak to average power ratio in ofdm systems,” in *WCNC. 1999 IEEE Wireless Communications and Networking Conference (Cat. No. 99TH8466)*, vol. 3, pp. 1095–1099, IEEE, 1999.
- [13] S. H. Müller and J. B. Huber, “Ofdm with reduced peak-to-average power ratio by optimum combination of partial transmit sequences,” *Electronics Letters*, vol. 33, no. 5, pp. 368–369, 1997.
- [14] A. D. Jayalath and C. Tellambura, “Reducing the peak-to-average power ratio of orthogonal frequency division multiplexing signal through bit or symbol interleaving,” *Electronics Letters*, vol. 36, no. 13, pp. 1161–1163, 2000.
- [15] J. Tellado, “Peak to average power reduction for multicarrier modulation,” *Stanford University, Ph. D. dissertation*, 2000.
- [16] B. S. Krongold and D. L. Jones, “Papr reduction in ofdm via active constellation extension,” *IEEE Transactions on broadcasting*, vol. 49, no. 3, pp. 258–268, 2003.
- [17] C. Li, T. Jiang, Y. Zhou, and H. Li, “A novel constellation reshaping method for papr reduction of ofdm signals,” *IEEE Transactions on Signal Processing*, vol. 59, no. 6, pp. 2710–2719, 2011.
- [18] M. Kim, W. Lee, and D.-H. Cho, “A novel papr reduction scheme for ofdm system based on deep learning,” *IEEE Communications Letters*, vol. 22, no. 3, pp. 510–513, 2017.
- [19] O. Russakovsky, J. Deng, H. Su, J. Krause, S. Satheesh, S. Ma, Z. Huang, A. Karpathy, A. Khosla, M. Bernstein, et al., “Imagenet large scale visual recognition challenge,” *International journal of computer vision*, vol. 115, no. 3, pp. 211–252, 2015.
- [20] J. Kim and Y. Shin, “An effective clipped companding scheme for papr reduction of ofdm signals,” in *2008 IEEE International Conference on Communications*, pp. 668–672, 2008.